

Published in final edited form as:

Am J Physiol Cell Physiol. 2007 May ; 292(5): C1880–C1886.

Recruitment of NADH Shuttling in Pressure Overloaded and Hypertrophic Rat Hearts

E. Douglas Lewandowski^{1,2}, J. Michael O'Donnell^{1,2}, Thomas D. Scholz³, Natalia Sorokina^{1,2}, and Peter M. Buttrick²

¹ Program in Integrative Cardiac Metabolism, University of Illinois at Chicago, College of Medicine, Chicago, IL 60612

² Center for Cardiovascular Research, University of Illinois at Chicago, College of Medicine, Chicago, IL 60612

³ Department of Pediatrics, University of Iowa, Iowa City, IA 52242

Abstract

Glucose metabolism in the heart requires oxidation of cytosolic NADH from glycolysis. This study examines shuttling reducing equivalents from the cytosol to the mitochondria via the activity and expression of the oxoglutarate-malate carrier (OMC), in rat hearts subjected to 2 (HYP2, n=6) and 10 weeks (HYP10, n=8) of pressure overload vs. that of sham-operated rats (SHAM2, n=6 and SHAM10, n=7). Moderate aortic banding produced increased atrial natriuretic factor (ANF) mRNA expression at 2 and 10 weeks, but only at 10 weeks did hearts develop compensatory hypertrophy (33% increase, $P < 0.05$). Isolated hearts were perfused with the short chain fatty acid, [2,4-¹³C₂] butyrate (2 mM) and glucose (5 mM) to enable dynamic-mode ¹³C NMR of intermediate exchange across OMC. OMC flux increased prior to development of hypertrophy: HYP2 = 9.6 ± 2.1 micromole/min/g dw vs. SHAM2 = 3.7 ± 1.2 providing an increased contribution of cytosolic NADH to energy synthesis in the mitochondria. With compensatory hypertrophy, OMC flux returned to normal: HYP10 = 3.9 ± 1.7 micromole/g/min vs. SHAM10 = 3.8 ± 1.2 . Despite changes in activity, no differences in OMC expression occurred between HYP and SHAM. Elevated OMC flux represented augmented cytosolic NADH shuttling, coupled to increased nonoxidative glycolysis, in response to hypertrophic stimulus. However, development of compensatory hypertrophy moderated the pressure-induced elevation in OMC flux, which returned to control levels. The findings indicate that the challenge of pressure overload increases cytosolic redox state and its contribution to mitochondrial oxidation, but that hypertrophy, prior to decompensation, alleviates this stress response.

Keywords

Malate-aspartate shuttle; redox state; hypertrophy

INTRODUCTION

Chronic pressure overload, such as that produced by hypertension, results in the development of cardiac hypertrophy, a pathophysiological response that has been linked to increased glucose metabolism (9,17,22,24). Increased reliance on glucose metabolism for energy synthesis in the hypertrophied myocardium requires an elevated oxidation of cytosolic NADH that is produced

from glycolysis (9,17,22,24). Under normal oxidative conditions, the reducing equivalents that are transferred to NAD^+ to form NADH in the cytosol can be transferred to the mitochondrial matrix in support of oxidative phosphorylation (2,23). This transfer of reducing equivalents from cytosolic NADH (NADHc) to the oxidative pathways of the mitochondria is achieved primarily via net forward flux through the malate-aspartate shuttle. Therefore, the present study examines the potential for augmented shuttling of reducing equivalents in hypertrophic hearts.

We have recently demonstrated that the neonatal heart, which is more glycolytically active than adult heart, adjusts to a relatively high level of glycolytic NADH production through elevated transfer rate of these cytosolic reducing equivalents into mitochondria via malate-aspartate shuttle flux (7,15). In that previous study, we observed that the increased malate-aspartate shuttle activity in the neonatal heart is supported by a relatively high level of expression of the shuttle protein, oxoglutarate-malate carrier (OMC) protein. As the developing heart reduces reliance on glucose metabolism during the shift to the adult metabolic profile of increased fatty acid oxidation, the myocardium reduces expression of both the malate-aspartate shuttle and glycerophosphate shuttle proteins, with essential elimination of the glycerophosphate shuttle (7,26). Consequently, the malate-aspartate shuttle proteins eventually provide the predominant form of reducing equivalent transfer in adult myocardium, albeit at a reduced capacity from the neonatal stage. Indeed, in the adult heart both flux through OMC and expression of the protein are reduced to approximately one-third of those seen in the neonatal heart (7). With the potential for the hypertrophic stimulus to initiate a reversion to neonatal metabolism, this study addresses the hypothesis that the hypertrophic heart, in shifting toward increased glucose metabolism, must adapt to the NADH/NAD⁺ balance of the cytosol through adjustments in OMC activity and/or expression.

To address this hypothesis, we employed dynamic-mode ^{13}C NMR to measure flux across the primary transporter protein involved in the transfer of NADHc into the mitochondrial matrix, OMC, in pressure loaded rat hearts (7,18,30). Our objectives were to 1) determine adaptive changes in flux across OMC and OMC protein expression in response to the hypertrophic stimulus of pressure overload and 2) examine OMC activity and expression in hearts at the point of development of compensatory hypertrophy. This study is the first to investigate altered mitochondrial transport processes in intact hypertrophic hearts and importantly, demonstrate the distinctions between metabolic regulation and gene expression in the adaptive responses to a disease process.

MATERIALS AND METHODS

Pressure-overload cardiac hypertrophy

Pressure-overload hypertrophy (HYP) was produced in hearts of male Sprague-Dawley rats by constriction of the transverse aorta as previously described (4). Hearts were harvested from age-matched, aortic banded and sham-operated rats for perfusion experiments at two time points: 1) at 2 weeks post-banding (6 weeks of age), prior to development of hypertrophy, but when elevated atrial natriuretic factor (ANF) mRNA expression confirmed the presence of a hypertrophic stimulus (5 fold increase over shams, $P < 0.05$), and 2) at 10 weeks post-banding (14 weeks of age), when established compensatory hypertrophy was evident. The protocol was approved by the Animal Care Policies and Procedures Committee at UIC (IACUC accredited), and animals used were maintained in accordance with the *Guide for the Care and Use of Laboratory Animals* (National Research Council, revised 1996).

Isolated perfused rat heart

Animals were heparinized (500 U/100 g ip.) and anesthetized with sodium pentobarbital (100 mg/kg i.p.). Hearts were excised and perfused in retrograde fashion at 100 cm hydrostatic

pressure, as previously described, with modified Krebs-Henseleit buffer (116 mM NaCl, 4 mM KCl, 1.5 mM CaCl₂, 1.2 mM MgSO₄ and 1.2 mM NaH₂PO₄, equilibrated with 95% O₂/5% CO₂) (7,18,30). A water-filled latex balloon was fitted into the left ventricle for hemodynamic recordings (PowerLab, AD Instruments, Colorado Springs, CO). The balloon was inflated with water to create a diastolic pressure of 5–10 mmHg. Left ventricular developed pressure (LVDP) and heart rate (HR) were continuously recorded. Rate-pressure product (RPP) was calculated as the product of heart rate and developed pressure. The temperature of the hearts was continuously maintained at 37°C.

Experimental Protocols

At the start of each protocol the perfusate supply was switched to a 0.5 liter reservoir of buffer containing 2.0 mM unlabeled butyrate and 5mM glucose for 10 minutes to ensure metabolic equilibrium and for collection of background signals of naturally abundant ¹³C (1.1%). During this period, a ³¹P spectrum was also acquired from each heart. The perfusate was then switched to a 1 liter supply of ¹³C-enriched buffer containing 2.0 mM [2,4-¹³C₂] butyrate (Isotec, Inc., Miamisburg, OH) plus 5mM unlabeled glucose. Sequential ¹³C NMR spectra began immediately upon delivery of ¹³C-enriched over 35 minutes (7,18,30). The heart was rapidly frozen in liquid nitrogen-cooled tongs for *in vitro* analysis.

Butyrate is a short chain fatty acid that undergoes beta-oxidation in cardiac mitochondria. Though not a physiological substrate, butyrate supports normal cardiac energetics and function and enables NMR measurements of metabolic flux in the intact beating heart (11,13,19,29, 30). Prior studies on OMC activity in the neonatal heart have employed butyrate to match OMC expression to activity (7). Therefore, ¹³C enriched butyrate was used as a probe of oxidative activity in the heart, enabling this protocol to focus on adjustments in OMC activity in the hypertrophied heart, without the potentially confounding variables associated with changes in long chain fatty acid entry into oxidative metabolism via the expression and activity of carnitine palmitoyl transferase I.

Four experimental groups of hearts were studied: 1) 2 weeks pressure-overload (n = 6); 2) age-matched, 2-week post-operative shams (n = 6); 3) 10 weeks pressure-overload (n= 8); 4) age-matched, 10-week post-operative shams (n = 7).

These protocols were mirrored using additional hearts perfused with 2 mM unlabeled butyrate plus 5 mM [1,6-¹³C₂] glucose to discern potential differences in the utilization of exogenous glucose versus unlabeled, endogenous carbohydrate. Heart were freeze clamped after 30 minutes and analyzed for the extent of glucose metabolism in the following groups: 1) 2 weeks pressure-overload (n = 5); 2) age-matched, 2-week post-operative shams n = 5); 3) 10 weeks pressure-overload (n= 6); 4) age-matched, 10-week post-operative shams (n = 5).

NMR measurements

NMR parameters required for acquisition of ³¹P and ¹³C NMR spectra from isolated hearts are as previously reported (7,11,18,19,30). Perfused hearts were positioned in a 20-mm broadband probe in a 9.4T/89-mm vertical-bore superconducting NMR magnet. ¹³C spectra were then acquired with bi-level broadband decoupling and subtracted from naturally abundant endogenous ¹³C signal. ³¹P spectra were acquired over a 2 minute time period.

High-resolution ¹³C and ¹H NMR spectra of perchloric acid extracts reconstituted in 0.5 ml ²H₂O were obtained with a 5-mm probe placed in a Bruker 14 T magnet as previously reported (13,29). The multiplet structures of the glutamate carbon signals allowed the fraction of [2-¹³C] labeled acetyl-CoA entering the tricarboxylic acid (TCA) cycle to be calculated

(10,16). ^1H NMR spectra and UV spectrophotometric assay, allowed determination of the glycolytic production of alanine and lactate.

Kinetic modeling of ^{13}C labeling of glutamate

Kinetic analysis of the ^{13}C enrichment curves for the 4- and 2-carbon positions of glutamate was performed by least squares fitting curves to a well established model (14,29,31). As shown in Figure 1, label from $[2,4-^{13}\text{C}_2]$ butyrate enters the TCA cycle as $[2-^{13}\text{C}]$ acetyl-CoA. Oxoglutarate is first labeled at the C4 position and then with equal probability at the C2 and C3 positions on the second turn of the TCA cycle. The interconversion of mitochondrial oxoglutarate with the NMR detectable pool of cytosolic glutamate is dominated by the rate-determining exchange of oxoglutarate across the mitochondrial membrane via OMC. Kinetic analysis of isotope data provided flux through the TCA cycle (V_{tca}) and through OMC (F_1) which dominates the interconversion rate of oxoglutarate and glutamate (7,14,29,30,31).

Biochemical analysis of metabolite concentrations and enzyme activities

Tissue was assayed for citrate, aspartate, glutamate, and oxoglutarate using UV and fluorometric techniques (1,28). ANF mRNA expression was determined as previously reported (6). OMC expression was measured by Western blotting of the 31 kD subunit as described by Scholz and colleagues (22,26). In order to assure that signals were in the linear detection range, variable exposures or serial dilutions were performed (data not shown).

Statistical comparisons

Results are reported as mean \pm standard deviation, unless otherwise indicated. Comparison of mean values was performed using Analysis of Variance followed by a Neuman-Keuls post-hoc test. Functional measurements over time were compared using the Repeated Measures Analysis of Variance. Differences in mean values were considered significant at a probability level of $<5\%$.

RESULTS

Pathophysiological and Bioenergetic States of Pressure Overloaded Rat Heart

Significant increases in the mean expression of atrial natriuretic factor (ANF) mRNA relative to GAPDH (dimensionless units) were present in hearts after aortic banding in comparison to sham operated rats (2-week sham = $1,191 \pm 259$ vs. 2-week banded = $5,008 \pm 758$; 10-week sham = $1,762 \pm 986$ vs. 10-week banded = $3,446 \pm 752$). However, compensatory hypertrophy was only evident after 10 weeks of pressure overload. Heart weight was similar between 2 week pressure overloaded hearts (1.7 ± 0.2 g) and corresponding shams (1.5 ± 0.2 g). The ratio of heart weight to body weight was also similar between 2 week pressure overloaded hearts (0.0065 ± 0.002) and corresponding shams (0.0069 ± 0.001). Heart weight was increased in 10 week pressure overloaded hearts (2.8 ± 0.3 g) over that of corresponding shams (2.1 ± 0.1 g, $P < 0.05$) and heart weight to body weight ratios were significantly increased in the banded animals at this time point (0.0071 ± 0.0004) as compared to shams (0.0051 ± 0.0005 , $P < 0.05$). Thus, we were able to study hearts at two key time points: 1) early after the imposition of the hypertrophic stimulus prior to the development of cardiac hypertrophy, and 2) once compensatory cardiac hypertrophy had been established.

Rate pressure product was similar in all four experimental groups and did not vary significantly throughout the perfusion protocol. RPP values (bpm \times mm Hg) at the mid point of the protocol were as follows: 2-week sham = $29,778 \pm 7,804$; 2-week banded = $28,843 \pm 6,238$; 10-week sham = $26,173 \pm 7,798$; 10-week banded = $22,323 \pm 3,829$ (Mean \pm SD). The pressure overloaded hearts at both 2 and 10 weeks showed no significant functional deficiency as compared to the

corresponding sham operated hearts. As hearts in the 10 week group had no evidence of hemodynamic decompensation or failure, the functional similarities between the pressure overloaded hearts and the sham operated hearts are to be expected.

Correspondingly, oxygen consumption was similar in all groups: 2-week sham = 22.0 ± 4.3 micromole/g/min; 2-week banded = 24.1 ± 5.2 ; 10 week sham = 23.8 ± 4.8 ; 10 week banded = 19.3 ± 3.4 . Consistent with previous reports, banded hearts at 10 weeks of pressure overload displayed reduced energy potential, as indexed by the ratio of phosphocreatine (PCr) to ATP (4,12): 2 week sham = 1.91 ± 0.25 vs. 2 week banded = 1.59 ± 0.39 (NS); 10 week sham = 1.98 ± 0.29 vs. 10 week banded = 1.62 ± 0.27 ($P < 0.05$).

Metabolic Flux Measurements and OMC Activity

Representative ^{13}C NMR spectra of the intact beating hearts, oxidizing [2,4- $^{13}\text{C}_2$] butyrate, are shown in Figure 2 with ^{13}C enrichment curves of the glutamate carbon positions, as described in the methods section above, shown in Figure 3. Isotopic steady state within the glutamate pool was reached within the first 20 minutes of the enrichment protocol as previously observed (7,19,29). Measured input parameters for the analysis of glutamate enrichment kinetics are shown in Table 1. Glutamate content in myocardium of hearts at 2 weeks pressure overload was increased, as expected due to an increase in OMC activity (18).

When the differences in metabolite pool size are accounted for with respect to the differences in the relative enrichment rates of the 2- and 4-carbon of glutamate, as is performed in the fitting of the data to the kinetic model (See Figure 3), the output from the kinetic model yielded the distinction in flux values shown in Figure 4. Measurements of TCA cycle flux in each group showed similar flux rates among all four experimental groups, as would be predicted by the similar functional performance of each group of hearts. Mean values of TCA cycle flux in each group were as follows: 2-week sham = 9.8 ± 4.0 micromole/min/g dry weight; 2-week banded = 8.3 ± 0.9 (NS); 10-week sham = 10.6 ± 4.1 ; 10-week banded = 10.2 ± 1.9 (NS).

OMC activity (F_1) in the intact, beating heart was essentially doubled in response to the hypertrophic stimulus at 2 weeks post-banding (Figure 4). Interestingly, OMC flux returned to near baseline levels at the time of significant compensatory hypertrophy. As anticipated, flux through OMC remained unchanged over the 2 to 10 week period in the sham operated, control hearts. These findings suggest that the OMC flux response is adaptive to the stimulus of pressure overload and normalizes upon compensation of the left ventricle.

As expected from the inhibitory effects of short chain fatty acid on carbohydrate oxidation, very little glucose was oxidized in the presence of butyrate as an oxidizable substrate (5,8, 27,30). Interestingly though, nonoxidative glycolysis as indicated by an increase in glycolytic end product formation (lactate and alanine), particularly that of lactate, was higher in the 2 week banded group than in the corresponding 2 week sham group (Table 1). Indeed, the 2 week banded group was the only set displaying elevated lactate content ($P < 0.01$). This finding is consistent with increased drive of the malate-aspartate shuttle via elevated cytosolic redox state in the 2 week banded group, as linked to the observed increased flux through OMC (23,30). While a general increase in glycolysis was evident in the pressure overloaded hearts, no distinctions were evident in the fate of the exogenous, enriched glucose versus the endogenous, unlabeled glucose.

OMC Expression in Pressure Overloaded Hearts

Despite increased metabolite exchange via OMC in hearts at two-weeks of pressure overload relative to sham hearts, OMC protein expression remained unchanged (Figure 5). Hearts subjected to ten-weeks of pressure overload showed mean OMC protein slightly elevated

(30%) over sham hearts, though not significantly. These results are similar to the findings reported by Rupert et al (22). However, previous studies were not able to evaluate flux through this transporter protein in the hypertrophied heart.

The present results indicate that OMC activity is significantly elevated due to metabolic regulation in the hearts at 2 weeks of pressure overload, prior to the development of compensatory hypertrophy, without any increase in protein expression. As compensatory hypertrophy develops, OMC flux returns toward baseline levels, despite no increase in the amount of OMC protein.

DISCUSSION

This study is the first to evaluate the activity of a key component of the malate-aspartate shuttle in heart in response to the hypertrophic stimulus. The work also represent the first dynamic ^{13}C NMR study of cardiac hypertrophy with actual metabolic flux measurements from sequential ^{13}C spectra of the beating heart. The major finding is that the early response to pressure overload includes increased flux through OMC which then moderates over time, coordinate with the development of compensatory hypertrophy. We previously demonstrated in a developmental model of cardiac metabolism, comparing neonatal hearts to adult hearts with similar methods, that the activity of OMC can be directly related to the level of OMC expression (7). However, in contrast to the previous study, the pressure-overloaded adult heart demonstrates similar regulatory responses of cardiac metabolism, but in the absence of altered enzyme expression. Importantly, this study demonstrates further that the metabolic response to pressure overload is an intrinsic adaptation in the myocardium, that persists in the isolated heart.

The ^{31}P NMR data showing depressed energetic profile in hearts of these aortic banded animals is consistent with previous reports of cardiac energetics in hypertrophy (4,17). PCr:ATP was equally perturbed at both 2 and 10 weeks of pressure overload and, as a general characteristic of the hypertrophic heart, did not correlate to OMC flux.

In cardiac hypertrophy, a phenotypic reprogramming occurs in the heart, such that genes that are normally expressed during development are recapitulated, including gene encoding metabolic enzymes (21). Metabolic studies on hypertrophied hearts have clearly documented an increase in glycolytic energy production in comparison to that of the normal heart (9,24). This shift is consistent with reversion to fetal gene expression program that was initially characterized for genes encoding myocyte contractile proteins (20,25). While we have observed a clear increase in the activity of OMC in the pressure-overloaded rat heart, protein levels did not revert to the fetal expression pattern that would present significantly elevated OMC expression either upon the onset of the hypertrophic stimulus or at the point of compensatory hypertrophy. The sole drive for increased OMC flux then appears to be due to increased glycolytic activity, as shown increased lactate and alanine content in the 2-week banded group.

Interestingly, the net appearance of NADH in the mitochondrial matrix which occurred through the sum of both NADH production via TCA cycle flux and NADH transfer from the cytosol were well matched in both sham and banded heart groups at 2 weeks to support similar levels of contractile function. The general production of 3 NADH per single cycle of the TCA pathway indicates that the mean TCA cycle flux for sham hearts, of 9.8 micromol/min/g, produced 29.4 NADH units per min/g, while the mean TCA cycle flux of 8.3 micromol/min/g in the banded group produced 24.9 NADH/min/g. However, the different contributions of NADH influx into the mitochondria via OMC activity brings the mean values of NADH generation in the mitochondria to very similar levels of 33.1 NADH/min/g in the sham group and 34.5 NADH/

min/g in the 2 week banded group. Thus, the similarity in total NADH contributing to oxidative energy synthesis in the mitochondria accounts for the observed similarities in oxygen consumption observed in both the sham and pressure overload hearts. The importance of this finding is that in the 2 week pressure overloaded heart, glycolytic production of NADH contributed significantly to maintaining normal rates of energy synthesis and this contribution diminished with the eventual development of compensatory hypertrophy.

Indeed, though statistical comparison does not indicate significance, the trend for OMC protein content in compensated hypertrophic myocardium was an increase by one third the amount of protein in the sham hearts. In this case, the relative flux through OMC per quantity of OMC protein in the heart remains elevated even in the 10-week banded animals. Therefore, the large increase in OMC flux prior to the development of compensatory hypertrophy represents an adjustment in metabolic regulation in response to the hypertrophic stimulus.

The elevated flux through OMC then becomes an important adaptive mechanism that serves to maintain cytosolic redox state (NADH/NAD⁺) in the presence of a previously reported mismatch between the elevated glycolytic activity of the hypertrophied and the relatively unchanged oxidation of glycolytic end products (9,24). Importantly, these observations of increased OMC flux and glycolytic metabolism occurred in hearts subjected to the stress of pressure overload, prior to the development of hypertrophy. Though the present study focuses not on glucose metabolism, but rather on the activity of the key transporter for cytosolic reducing equivalents OMC, our data on the ¹³C enrichment of acetyl CoA (Table 1) demonstrate no differences between sham hearts and pressure overloaded hearts in the relative contributions to oxidative metabolism between butyrate and glucose. Therefore, no increase in the oxidation of glycolytic end products was observed in this study of pressure overloaded hearts, supporting the previously reported findings (9,24).

Although the aim of this study was the measurement of flux through OMC that precluded measurements of glycolytic flux, these new data build on the previously published reports of changes in the intermediary metabolism of the hypertrophied rat heart (9,17,22,24). The findings of this study indicate that shortly after imposition of the hypertrophic stimulus of pressure overload, flux through OMC is dramatically increased in the heart, as reducing equivalent transfer from the glycolytically produced, cytosolic NADH is accommodated by the malate-aspartate shuttle for oxidative metabolism in the mitochondria. Evidence is shown here for a transient spike in the activity of non-oxidative glycolysis that is a likely culprit for driving OMC. As the early elevation of glycolysis has been observed in the isolated heart, it represents an intrinsic change in myocardial metabolism.

Interestingly, once compensation occurs after 10 weeks of pressure overload, the flux through OMC returns toward baseline levels, similar to those observed in the sham hearts. Together, data from both the 2- and 10-weeks time points of pressure overload indicate that development of compensatory hypertrophy at least partially restores the redox state balance (NADH/NAD⁺) between the cytosol and mitochondria, which is initially disrupted during the initial metabolic response to pressure overload.

Our further analysis of OMC content in pressure overloaded hearts indicates that the changes in OMC flux, that were observed in this study, are the direct result of metabolic regulation and not a change in the expression of the enzyme. While we have observed a clear increase in the activity of OMC in the pressure overloaded heart (at 2 weeks), protein levels did not revert to the fetal expression pattern (7). An earlier study, by Rupert, et al (22), also demonstrated that protein levels of OMC do not increase in rat heart following pressure overload produced by banding the abdominal aorta.

Nonetheless, the lack of change in OMC content in response to the hypertrophic stimulus belies the altered activity of this carrier protein and the changes in OMC activity that occur in parallel with the development of compensatory cardiac hypertrophy. The results show, in general, that the metabolic responses to pressure overload in the heart are not static. Rather, the initial spike in OMC activity and eventual moderation toward baseline activity in hypertrophic hearts suggests that meeting the metabolic demands of cardiac function is a dynamic process over the course of the pathophysiology that ultimately leads toward decompensated hypertrophy and heart failure. Indeed, this process clearly adapts to the current pathophysiological state and may induce subsequent adaptive responses, that do not involve distinct changes in enzyme expression. The larger implication of the work is that *in vitro* assays that rely primarily on enzyme content or enzyme kinetics, in the absence of the metabolic driving forces provided by the function of the intact ventricle, do not reflect the regulatory control of metabolic processes in the cardiomyocyte.

Acknowledgements

This work was supported in part by the National Institutes of Health Grant RO1HL62702, R37HL49244, and HL P0162426.

References

1. Bergmeyer, HU. *Methods in enzymatic analysis*. Verlag-Chemie International; Deerfield Beach, FL: 1974. p. 2308
2. Cederbaum AI, Lieber CS, Beattie DS, Rubin E. Characterization of shuttle mechanisms for the transport of reducing equivalents into mitochondria. *Arch Biochem Biophys* 1973;158:763–781. [PubMed: 4782532]
3. Damico LA, White LT, Yu X, Lewandowski ED. Chemical versus isotopic equilibrium and the metabolic fate of glycolytic end products in the heart. *J Mol Cell Cardiol* 1996;28:989–999. [PubMed: 8762037]
4. DelMonte F, Williams E, Lebeche D, Schmidt U, Rosenzweig A, Gwathmey JK, Lewandowski ED, Hajjar RJ. Improvement in Survival and Cardiac Metabolism Following Cardiac-Specific Gene Transfer of 3ORCA2a in an Animal Model of Heart Failure. *Circulation* 2001;104:1424–1429. [PubMed: 11560860]
5. Dennis SC, Padmas A, DeBuysere MS, Olson MS. Studies on the regulation of pyruvate dehydrogenase in the isolated perfused rat heart. 1979;254:1252–1258.
6. Goldspink P, Montgomery D, Walke LA, Urboniene D, McKinney RD, Geenen DL, Solaro RJ, Buttrick PM. PKC-epsilon over-expression alters cardiac myofilament properties and composition during the progression to heart failure. *Circ Res* 2004;95:424–34. [PubMed: 15242976]
7. Griffin J, O'Donnell JM, White LT, Hajjar RJ, Lewandowski ED. Postnatal expression and activity of the 2-oxoglutarate malate carrier in intact hearts. *Am J Physiol: Cell Physiology* 2000;279:C1704–C1709.
8. Johnston DL, Lewandowski ED. Fatty acid metabolism and contractile function in the reperfused myocardium: multinuclear NMR studies of isolated rabbit hearts. *Circ Res* 1991;68:714–725. [PubMed: 1742864]
9. Leong HS, Brownsey RW, Kulpa JE, Allard MF. Glycolysis and pyruvate oxidation in cardiac hypertrophy – Why so unbalanced? *Comp Biochem and Physiol* 2002;135:499–513.
10. Lewandowski ED, Doumen C, White LT, LaNoue KF, Damico LA, Yu X. Multiplet structure of ¹³C NMR signal from glutamate and direct detection of TCA cycle intermediates. *Magn Reson Med* 1996;35:149–154. [PubMed: 8622576]
11. Lewandowski ED, Chari MV, Roberts R, Johnston DL. NMR studies of β -oxidation and short chain fatty acid metabolism during recovery of reperfused hearts. *Am J Physiol (Heart and Circ Physiology)* 1991;261:H354–H363.
12. Lewandowski ED, Johnston DL, Roberts R. Effects of inosine on glycolysis and contracture during myocardial ischemia. *Circulation Research* 1991;68(2):578–587. [PubMed: 1991356]

13. Lewandowski ED, Kudej RK, White LT, O'Donnell JM, Vatner SF. Mitochondrial preference for short chain fatty acid oxidation during coronary artery constriction. *Circulation* 2002;105:367–72. [PubMed: 11804994]
14. Lewandowski ED, Yu X, White LT, Doumen C, LaNoue KF, O'Donnell JM. Altered metabolite exchange between subcellular compartments in intact postischemic hearts. *Circ Res* 1997;81:165–174. [PubMed: 9242177]
15. Lopaschuk GD, Spafford MA, Marsh DR. Glycolysis is the predominant source of myocardial ATP production immediately after birth. *Am J Physiol* 1991;261:H1698–H1705. [PubMed: 1750528]
16. Malloy CR, Sherry AD, Jeffrey FMH. Evaluation of carbon flux and substrate selection through alternate pathways involving the citric acid cycle of the heart by ¹³C NMR spectroscopy. *J Biol Chem* 1988;265:6964–6971. [PubMed: 3284880]
17. Nascimben L, Ingwall JS, Lorell BH, Pinz I, Schultz V, Tornheim K, Tian R. Mechanisms for increased glycolysis in the hypertrophied rat heart. *Hypertension* 2004;44(5):662–667. [PubMed: 15466668]
18. O'Donnell JM, Doumen C, LaNoue KF, White LT, Yu X, Alpert NM, Lewandowski ED. Dehydrogenase regulation of metabolite oxidation and efflux from mitochondria of intact hearts. *Am J Physiol (Heart and Circ Physiol)* 1998;274:H467–H476.
19. O'Donnell JM, Alpert NM, White LT, Lewandowski ED. Coupling of Mitochondrial Fatty Acid Uptake to Oxidative Flux in the Intact Heart. *Biophys J* 2002;82:11–18. [PubMed: 11751291]
20. Parker TG. Molecular biology of cardiac growth and hypertrophy. *Herz* 1993;18:245–255. [PubMed: 8375804]
21. Razeghi P, Young ME, Alcorn JL, Moravec CS, Frazier OH, Taegtmeier H. Metabolic gene expression in fetal and failing human heart. *Circulation* 2001 Dec 11;104(24):2923–31. [PubMed: 11739307]
22. Rupert BE, Segar JL, Schutte BC, Scholz TD. Metabolic adaptations of the hypertrophied heart: role of the malate/aspartate and alpha-glycerophosphate shuttles. *J Mol Cell Cardiol* 2000;32:2287–2297. [PubMed: 11113004]
23. Safer B, Williamson JR. Mitochondrial-cytosolic interactions in perfused rat heart. Role of coupled transamination in repletion of citric acid cycle intermediates. *J Biol Chem* 1973;248:2570–2579. [PubMed: 4349041]
24. Sambanddam N, Lopaschuk GD, Brownsey RW, Allard MF. Energy metabolism in the hypertrophied heart. *Heart Failure Reviews* 2002;7:161–173. [PubMed: 11988640]
25. Schneider MD, Roberts R, Parker TG. Modulation of cardiac genes by mechanical stress. The oncogene signalling hypothesis. *Mol Biol Med* 1991;(2):167–183. [PubMed: 1839641]
26. Scholz T, Koppenhafer S. Reducing equivalent shuttles in developing myocardium: enhanced capacity in the newborn heart. *Pediatr Res* 1995;38:221–227. [PubMed: 7478820]
27. Weiss RG, Chacko VP, Gerstenblith G. Fatty acid regulation of glucose metabolism in the intact beating rat heart assessed by carbon-13 NMR spectroscopy: the critical role of pyruvate dehydrogenase. *J Mol Cell Cardiol* 1989;21:469–478. [PubMed: 2528640]
28. Williamson, JR.; Corkey, BE. Assays of intermediates of the citric acid cycle and related compounds by fluorometric enzyme methods. In: Colowich, JM., editor. *Methods in Enzymology*. New York: Academic; 1969. p. 434-514.
29. Yu X, White LT, Doumen C, Damico LA, LaNoue KF, Alpert NM, Lewandowski ED. Kinetic analysis of dynamic ¹³C NMR spectra: metabolic flux, regulation, and compartmentation in hearts. *Biophysical J* 1995;69:2090–2102.
30. Yu X, White LT, Alpert NM, Lewandowski ED. Subcellular metabolite transport and carbon isotope kinetics in the intramyocardial glutamate pool. *Biochemistry* 1996;35:6963–6968. [PubMed: 8639648]
31. Yu X, Alpert NM, Lewandowski ED. Modeling glutamate enrichment kinetics from dynamic ¹³C NMR spectra of hearts: Theoretical analysis and practical considerations. *Am J Physiol (Cell Physiology)* 1997;272:C2037–C2048.

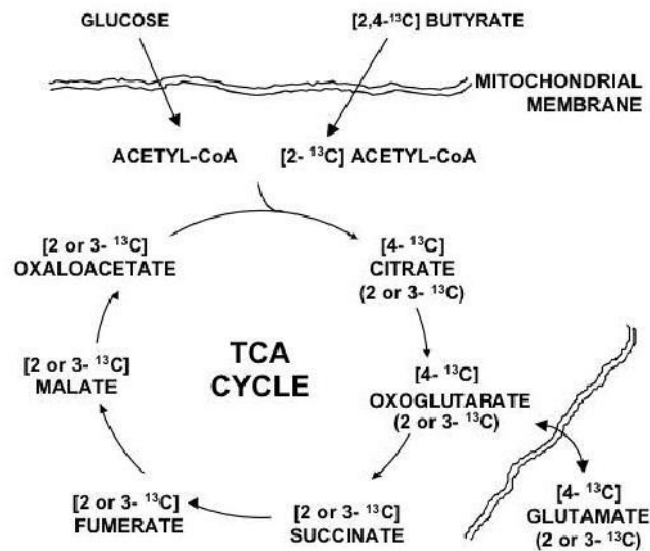


Figure 1.

Schematic diagram of metabolic processes probed with ^{13}C enriched butyrate and unlabeled glucose. ^{13}C enrichment of glutamate results after beta-oxidation of [2,4- $^{13}\text{C}_2$] butyrate produces [2- ^{13}C] acetyl CoA, which enters the TCA cycle, eventually enriching the intermediate, oxoglutarate. ^{13}C enriched oxoglutarate is exchanged with the glutamate pool, which is over 90% cytosolic. After initial ^{13}C enrichment of the TCA cycle intermediates at the 4-carbon site, the enrichment is recycled, appearing at the 2- and 3-carbon sites within the intermediates in equal probability. Unlabeled Acetyl CoA is also produced from unlabeled glucose which contributes pyruvate for oxidation via pyruvate dehydrogenase (PDH).

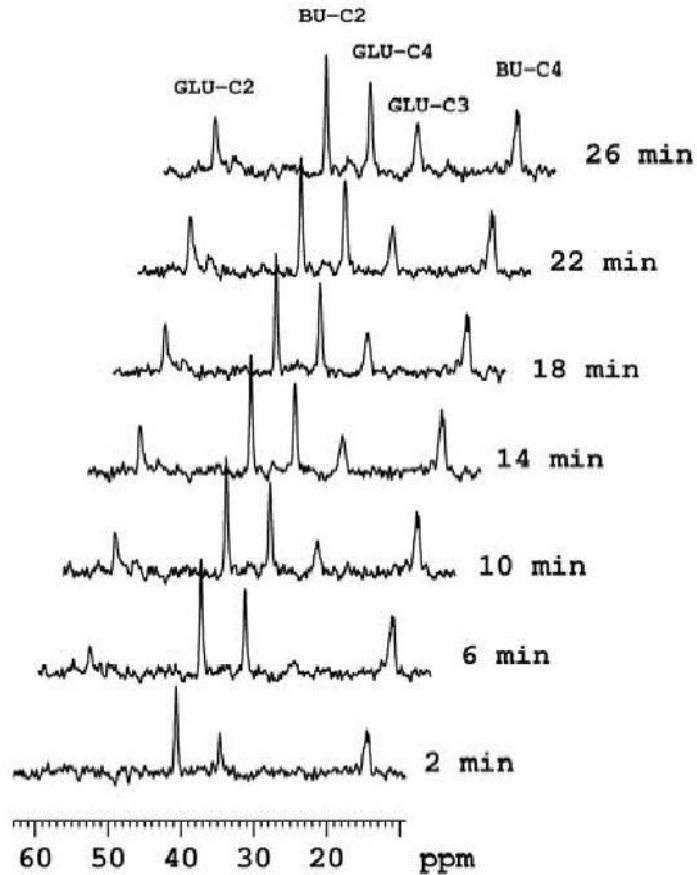


Figure 2. Selected ^{13}C spectra, each collected in 2 minute time periods, from a dynamic data set (from bottom to top) obtained from an isolated, hypertrophied rat heart (10 weeks pressure overload) perfused oxidizing $[2,4-^{13}\text{C}_2]$ butyrate in the presence of unlabeled glucose. Peak assignments are glutamate carbon-2 (GLU-C2), glutamate carbon-3 (GLU-C3), and glutamate carbon-4 (GLU-C4). BU-C2 and BU-C4 signals are from exogenous $[2,4-^{13}\text{C}_2]$ butyrate.

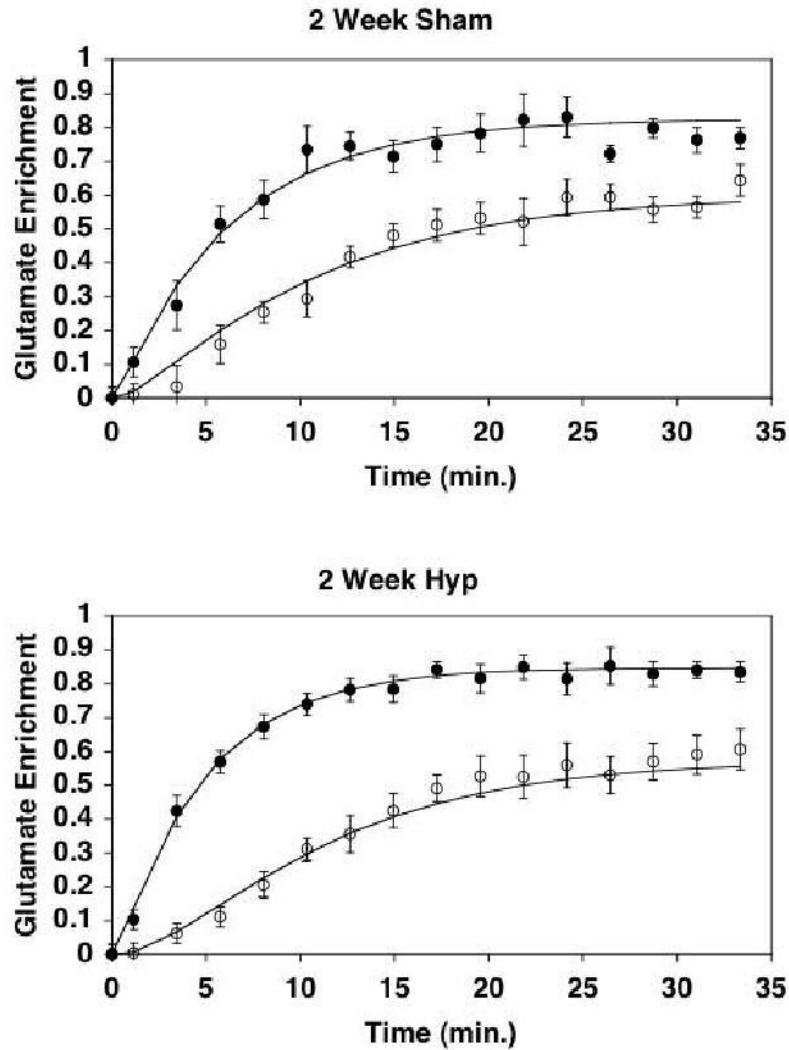


Figure 3. Mean (\pm SE) ^{13}C enrichment curves for the 4- and 2-carbon positions of glutamate, as detected by ^{13}C NMR. Solid line represents least squares fitting of the kinetic model to the enrichment data. Closed circles, 4-carbon of glutamate; Open circles, 2-carbon of glutamate. Top Panel, Sham operated hearts at 2 weeks (SHAM); Bottom Panel, Pressure-overloaded hearts at 2 weeks (HYP). Note the relative differences between ^{13}C enrichment at the 2-carbon position of glutamate versus that of the 4-carbon between the sham-operated hearts (Top) and the pressure overloaded hearts (Bottom).

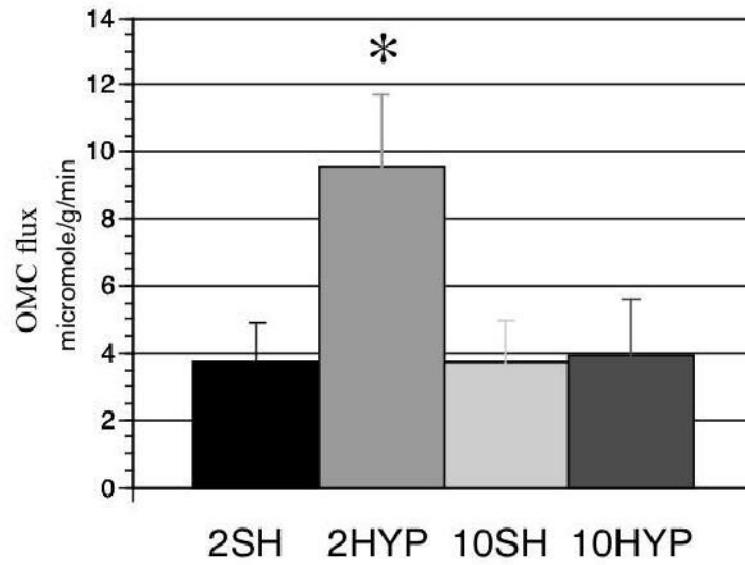


Figure 4.

Flux through the oxoglutarate-malate carrier (OMC) in each experimental group (micromole/min/g dry w). Groups values from left to right are identified as: 2SH, Sham operated hearts at 2 weeks; 10HYP, Pressure-overloaded hearts at 2 weeks; 10SH, Sham operated hearts at 10 weeks; 10HYP, Pressure-overloaded hearts at 10 weeks. Note significant increase in OMC activity at 2 weeks of pressure overload. *, $P < 0.0005$.

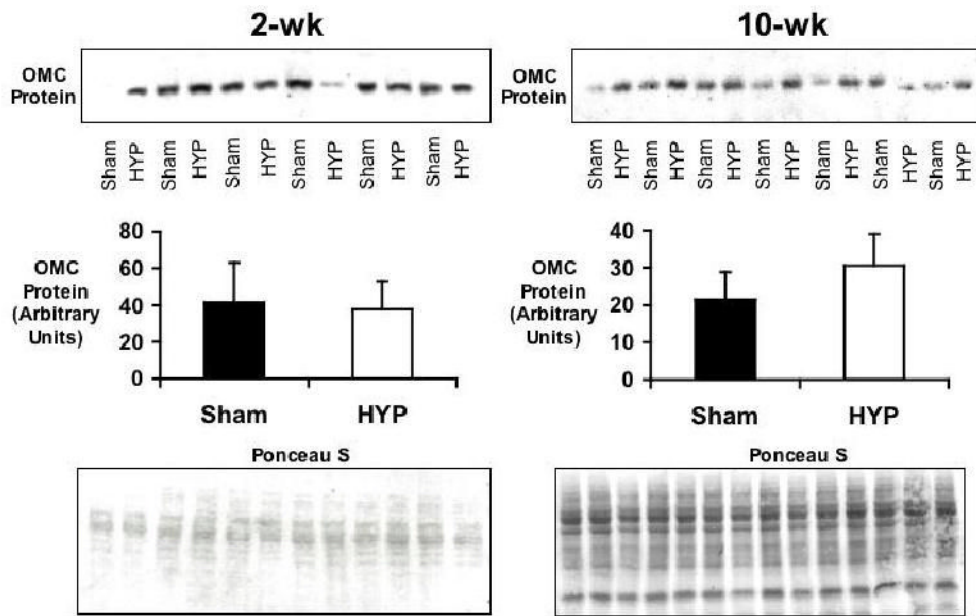


Figure 5. OMC protein levels in 2- and 10-week sham operated (Sham) and pressure-overloaded (HYP) hearts. Top panels display results of Western blots. Bar graphs indicate mean signal intensity (\pm SD). No significant difference in OMC levels was detected between Sham and HYP groups at the two time points. Bottom panels show results of ponceau staining to ensure uniform protein loading.

Table 1

Metabolic parameters for analysis of glutamate enrichment kinetics. Tissue metabolites are shown in micromole/g dry w (mean \pm SD).

Group	Glutamate	Citrate	Oxoglutarate	Aspartate	% ¹³ C acetyl-CoA	Lactate	Alanine
2 week Sham	19 \pm 4	2.3 \pm 0.1	0.21 \pm 0.08	5.6 \pm 1.3	85 \pm 1	2.3 \pm 1.9	0.7 \pm 0.6
2 week Banded	24 \pm 4 *	2.6 \pm 0.5	0.22 \pm 0.08	6.1 \pm 1.2	87 \pm 2	4.7 \pm 0.9 *	1.8 \pm 0.5 *
10 week Sham	16 \pm 5	3.2 \pm 1.2	0.17 \pm 0.03	4.6 \pm 1.3	89 \pm 3	2.5 \pm 1.5	1.1 \pm 0.7
10 week Banded	16 \pm 4	3.4 \pm 0.4	0.19 \pm 0.04	5.8 \pm 1.8	87 \pm 4	2.3 \pm 1.4	0.9 \pm 0.4

* , P<0.05 difference versus corresponding sham value.